Latin American Journal of Solids and Structures
www.lajss.org

# Effect of CFRP and TRM Strengthening of RC Slabs on Punching Shear Strength

**Abstract**

The paper presents experiments involving punching of RC slabs strengthened using externally bonded carbon fiber reinforced polymer (CFRP) sheet and textile reinforced mortar (TRM). Twelve RC slab specimens of two concrete grades (39.9 and 63.2 MPa) and employing two strengthening schemes (CFRP and TRM) were tested. Specimens were supported on two opposite edges. Experimental load-displacement variations show two peak loads in strengthened slabs and one peak followed by a plateau in control. Second peak or the plateau corresponds to the combined action of aggregate interlock and the dowel action of back face rebars and strengthening layers. The dowel action of back face rebars and strengthening layers had no role in ultimate punching load (i.e. first peak). Strengthened slabs showed 9-18% increase in ultimate punching load (i.e. first peak) whereas there was significant increase in the second peak load (190-276% for CFRP; 55-136% for TRM) and energy absorption (~66% for CFRP and 22-56% for TRM). An analytical model was also developed for predicting the punching shear strength (first and second peaks) of strengthened slabs showing good comparison with experiments.

**Keywords**

Punching; Slab; Concrete; Strengthened; CFRP; TRM; Dowel

**Husain Abbas*** [a]
**Aref A. Abadel** [a]
**Tarek Almusallam** [a]
**Yousef Al-Salloum** [a]

[a] Dept. of Civil Engineering, King Saud Univ., Riyadh 11421, Saudi Arabia.

*Author email:
abbas_husain@hotmail.com

http://dx.doi.org/10.1590/1679-78251277

Received 09.04.2014
In Revised Form 11.07.2014
Accepted 09.02.2015
Available Online 23.03.2015

## 1 INTRODUCTION

Punching shear failure of reinforced concrete (RC) slabs is a major concern for the structural designers of buildings and bridges. This type of failure is more common in bridge decks supported by girders under the action of repeated wheel loads (Meier, 1992; Hassanzadeh and Sundqvist, 1998; Malvar et al., 2000; Oh and Sim, 2004). The bridge decks are often strengthened for flexure by external bonding of Fiber Reinforced Polymer (FRP) sheets but the consequent enhancement in shear strength is generally low and not well known. Many previous studies have examined the punching

shear strength of FRP strengthened RC slabs; however, there are some theoretical deficiencies in the conventional theory, which are not able to explain the influence of FRP strengthening on punching resistance of RC slabs. Errors in predicting the punching shear capacity have been known to cause catastrophic failures resulting in huge loss of life and property. One such failure is the collapse of the six-year old, five-storey Sampoong Department store (originally designed as an office block and later converted to department store with reckless structural modifications) in Seoul, Korea in 1995. This collapse under service conditions led to several casualties (Gardner et al., 2002).

FRP materials are nowadays commonly used for the strengthening of structural RC elements (Elsanadedy et al., 2011; El-Sayed, 2014; Siddiqui, 2011). There are several studies on flexural strengthening of RC slabs using externally bonded FRP sheets (Meier, 1992; Kim and Sebastian, 2002; Limam et al., 2005; Al-Rousan et al., 2012; Ghali et al., 1974; Ebead and Marzouk, 2002; Adetifa and Polak, 2005). However, the FRP strengthening technique for punching shear failure is fairly new, with little research reported in this area (Erki and Heffernan, 1995; Malvar et al., 2000; Chen and Li, 2000; Wang and Tan, 2001; Van Zowl and Soudki, 2003; Cheng and Chung, 2005). Koppitz et al., (2013) reviewed the efficiency of available analytical models for predicting the punching shear strength of strengthened RC flat slabs and highlighted deficiencies in the models.

Erki and Heffernan (1995) used FRP sheets on the tension surface of RC slabs and observed that both flexural stiffness and punching shear capacity of the slabs improved while the flexural cracking was delayed. Wang and Tan (2001) investigated the punching shear behavior of RC flat slabs externally strengthened with carbon fiber-reinforced polymer (CFRP) sheets. The strengthened specimens with FRP sheets had an average of 8% increase in punching load over the control. Binici and Bayrak (2003) investigated the effectiveness of strengthening technique for increasing punching shear resistance in RC flat plates using CFRP strips. The results showed that the strengthening can shift the failure surface away from the column and the increase in the load carrying capacity was up to 51%. Harajli and Soudki (2003) investigated experimentally the shear capacity of two-way interior RC slab-column connections strengthened with CFRP sheets. They found that CFRP sheets on the tension face of the connection improved flexural and shear capacities by about 17–45%. The CFRP sheets did not change the location of punching shear failure surface significantly. Van Zowl and Soudki (2003) tested six slabs externally strengthened with CFRP sheets. The shear capacity increase for the CFRP strengthened slab was 29%. Ebead and Marzouk (2004) tested two-way slab-column connections to investigate the effect of using CFRP strips as an external strengthening technique against punching shear failure. The strengthened specimens had an average increase of 9% in the ultimate load capacity. El-Salakawy et al., (2004) used a combination of FRP sheets and steel bolts for shear strengthening of RC slabs and found increased connection ductility and ultimate strength along with a change in the failure pattern from the punching to the flexural mode. Esfahani et al., (2009) studied the punching shear strengthening of flat slabs using CFRP sheets which were located at the tension side of the slabs. The test results showed that the use of CFRP sheets, in addition to steel reinforcing bars, as flexural reinforcement improves the punching shear strength of slabs. This improvement can be significant for the slabs made of high strength concrete and low steel reinforcement ratio. Soudki et al., (2012) studied the effect of externally bonded CFRP strips on the punching shear of interior slab-column connections. The test results showed

that CFRP strengthening leads to significant improvements in the structural behaviour of slab-column connections. The increase in punching capacity of strengthened slabs was up to 29%, while the increase in stiffness was up to 80%. Abbas et al., (2004) studied the behavior of circular concrete plates strengthened with steel skin under drop hammer loading. Cantwell and Smith (1999) showed that the quasi-static and dynamic flexural strength of concrete can be greatly enhanced by bonding a relatively thin CFRP skin to the lower surface of beams.

Chen and Li (2005) used Glass Fiber Reinforced Polymer (GFRP) laminates for the shear strengthening of slabs. They showed that the flexural strengthening of slabs by external bonding of GFRP laminates can increase the punching strength, significantly. However, GFRP laminates were more effective for the slabs with low steel reinforcement ratios. They proposed analytical equations to calculate the punching strength of strengthened slabs. Abdullah et al., (2013) investigated the effectiveness of bonding non-prestressed and prestressed CFRP plates to the tension surface of RC column-slab connections in the strengthening of slabs. They found that the use of prestressed CFRP plates improved the serviceability but did not enhance the ultimate behavior as much as the non-prestressed CFRP plates. The development of the critical diagonal crack was the main reason for the reduction in the ultimate capacity of the strengthened slabs. Textile reinforced mortar (TRM) is emerging as a promising alternative to FRP for concrete applications due to the elimination of organic binders of FRP composites with inorganic ones i.e. cement-based mortar (RILIM TC 201TRC, 2006; Triantafillou, 2006; Triantafillou and Papanicolaou, 2006; Pled and Mobasher, 2007; Papanicolaou et al., 2009; Al-Salloum et al., 2011; Alhaddad et al., 2012; Arboleda et al., 2012). Textiles comprise fabric meshes made of long woven, knitted, or even unwoven fiber roving in at least two (typically orthogonal) directions. TRM was investigated in this study as a new method for the strengthening of concrete slabs. TRM used in this study consist of textile meshes made of carbon fibers roved in two directions and cement mortar serving as binder, containing polymeric additives.

Oh and Sim (2004) proposed an analytical model for predicting the punching shear strength of bridge decks strengthened using external strengthening techniques. The proposed punching shear model was used for predicting the ultimate shear strength of slabs strengthened using different materials. Sharaf et al., (2006) studied the effect of retrofitting interior slab–column connections against punching shear failure with externally bonded CFRP strips. The results show 29% to 60% increase in stiffness and 6% to 16% increase in punching capacity. An analytical model was refined to predict the punching shear capacity of the specimens strengthened with CFRP strips. Rochdi et al., (2006) developed an analytical model to predict the punching failure load of RC slabs with externally bonded FRP sheets based on the integration of the tensile stresses around the punching crack and the dowel effect of reinforcing bars and FRP sheet. Farghaly and Ueda (2011) investigated experimentally and analytically the punching shear capacity of CFRP strengthened two way slabs. The results showed up to 40% increase in the punching capacity of slabs. An analytical model was also developed for predicting the punching shear strength of strengthened RC slabs.

The above review shows that many previous studies have examined the punching shear strength of concrete slabs but there are still some theoretical deficiencies. Also the experimental research reported to date does not include theoretical punching shear analysis of the strengthened RC slabs

that is suited for adoption in practice with confidence. The paper studies the effect of CFRP and TRM strengtheneing of RC slabs, commonly adopted for their flexural strengthening, on the punching shear resistance of slabs and provides an analytical method for its prediction.

## 2 EXPERIMENTAL PROGRAM

The RC slabs of 600 × 600 × 90 mm size and reinforced with ϕ8@100 mm c/c bars (0.71% steel) were used in this study. The slabs were singly reinforced with rebars provided on the rear face of the slab. The reinforcement details of slabs are shown in Figure 1. Six slabs each were casted in two concrete grades thus making a total of twelve slab specimens. Two RC slabs of each group were taken as control whereas the remaining four slabs were strengthened using two different schemes of external strengthening. The materials used for strengthening were CFRP and TRM. The CFRP and TRM were applied on the rear face of slabs (Figure 1). The details of experimental program are given in Table 1.

Slab specimens of the two concrete grades A and B were cast in two separate batches. The specimens were cast in wooden moulds. The fabricated steel cages with cover blocks were placed in the mould. Concrete with 10 mm maximum size of aggregate and a slump of 18 mm was used for the casting of slabs. The casting was done in a single layer and compacted by a pin vibrator. Immediately after casting, screeding of top surface of the slab was done and then the slab specimens were covered with moist burlap and polythene sheets. Subsequently, the specimens were subjected to intermittent spraying of water every day for two weeks and then the form was removed and specimens were left to dry for the next two weeks. Three companion standard concrete cylinders (150 × 300 mm) were cast for each grade of concrete. The cylinders were cured in the water tanks for 28 days and tested in accordance with ASTM C39 (2012). The average compressive strength of concrete for the two grades was 39.9 and 63.2 MPa respectively. The rebars of 8 mm diameter were tested in accordance with ASTM A370 (2012) and the average yield strength was 510 MPa.

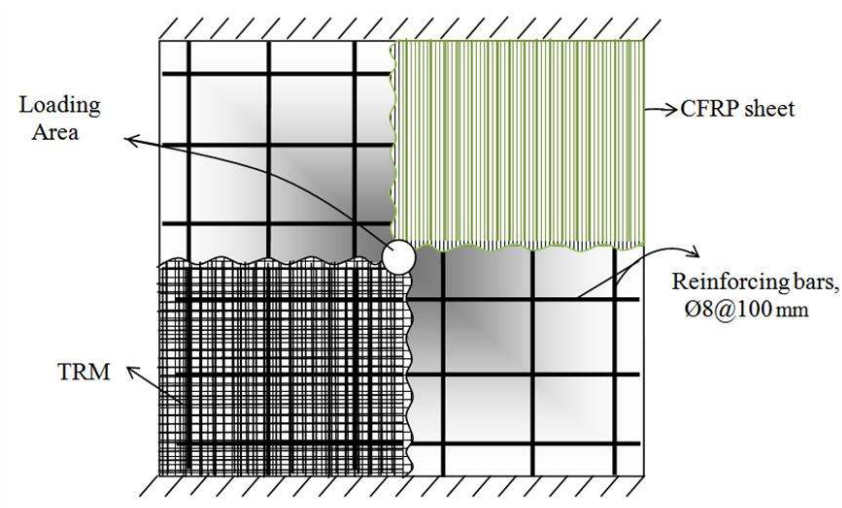


Figure 1: Reinforcement details of concrete slabs.

| Slab specimen ID | Concrete grade | Strengthening scheme |
|---|---|---|
| SA-1,2 | A | None |
| SA-C1,2 | A | Single sheet of unidirectional CFRP with fibers along span direction |
| SA-T1,2 | A | Two layers of bidirectional TRM |
| SB-1,2 | B | None |
| SB-C1,2 | B | Single sheet of unidirectional CFRP with fibers along span direction |
| | B | Two layers of bidirectional TRM |
| Total number of slab specimens = 12 | | |

Table 1: Test matrix.

### 2.1 CFRP System and Strengthening

The properties of composite materials are dependent on the individual components properties, the manufacturing technique and the quality control of the production process. In the present study, CFRP sheets with unidirectional fibers were employed for the strengthening of RC slab specimens. Three coupon samples were cut from the sheets to determine the average mechanical properties of the sheets. Each specimen was subjected to a gradually increasing uniaxial load until failure. The average coupon test results of CFRP system are:

| | |
|---|---|
| Elastic modulus of CFRP in primary fibers direction = | 77.3 GPa |
| Elastic modulus of CFRP $90^{o}$ to primary fibers = | 40.6 MPa |
| Fracture strain = | 1.1% |
| Ultimate Tensile strength = | 846 MPa |

Single layer of unidirectional CFRP with fibers along the span was used for the strengthening of slab specimens. The procedure adopted for affixing the CFRP layer to the slabs is shown in Figure 2.



a) Slab surface preparation

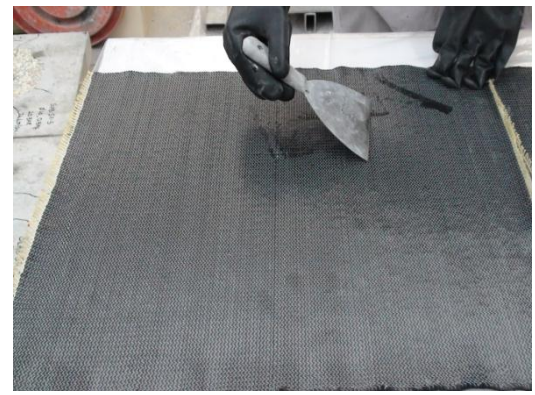

b) CFRP impregnation



c) CFRP sheet laying



d) Prepared specimens

Figure 2: Strengthening of slabs with externally bonded CFRP sheet.

## 2.2 TRM Materials and Strengthening

TRM consists of two primary materials namely Textile and Mortar. Success of rehabilitation using TRM is very much dependent on the properties of these two constituents of TRM.

The textile was cut to the required length. The textile contained equal quantity of high strength carbon fiber roving in two orthogonal directions. To obtain the mechanical properties of the textile, four coupons were tested in tension and the average test results are:

| | |
|---|---|
| Elastic Modulus of textile: | 33 GPa |
| Fracture strain of textile: | 0.95% |
| Ultimate tensile strength of textile: | 907MPa |
| Thickness per one textile layer, $t_f$ : | 0.2 mm |
| Width per one textile roving: | 3.93mm |
| Clear spacing between the roving: | 10 mm |

In the present study, a commercial polymer modified mortar was used as mortar in TRM strengthening. To prepare the mortar for the compressive strength test, 16-18% of drinking quality water (by weight of dry powder) was put in a dry bowl; mortar was added, and then it was mixed for 3 to 5 minutes until homogeneous mixture was obtained. Molding of the specimens was then done by placing a layer of mortar about 25 mm in thickness in the cube compartments. Each layer was tamped 32 times within 10 seconds in four rounds. After tamping of the first layer in all the cube compartments, the second layer was introduced and tamped in the same manner as above. Finally, top surface of cube compartment was smoothed off with one stroke of the trowel. The specimens were air dried for one-day and were de-molded; the specimens were then kept for water curing under lab conditions for 28 days. Standard compressive strength tests were conducted as per ASTM C109 (2002) at 28 days and the average compressive strength of mortar was 33.9 MPa.

In order to determine the tensile strength of the mortar, standard Briquette specimens were prepared having inside faces and thickness at waistline of the briquette mold as 25 mm. Briquette specimens for each mortar type using same amount of water as determined for compressive strength were prepared in accordance with ASTM C190-85 (1985). A thin film of oil was coated on the inside surfaces of the Briquette molds, and were placed on base plates. The molds were filled heaping full of mortar without any compacting. The mortars were pressed in firmly with the thumbs applying a force 12 times to each Briquette. Additional mortar was added above the molds, and smoothed it off with a trowel. Oiled metal plates were placed on top of each mold; bottom and top plates were held together with the hands and turned the molds over. The process of adding and pressing additional mortar above the molds, was repeated and smooth it off with a trowel. The specimens were air dried for one day. After one day of air drying, the specimens were de-molded and kept for curing under lab conditions. Before testing, each Briquette was wiped to surface-dry condition, and any loose sand grains from the surfaces were removed. Standard tensile tests were conducted at 28 days as per ASTM C190-85 (1985) and the average tensile strength of the mortar was 2.93 MPa.

Two layers of textile were used for TRM strengthening because two layers of textile were found equivalent to single layer of CFRP in an earlier study (Al-Salloum et al., 2011). The procedure adopted for affixing TRM to the slabs is shown in Figure 3.

### 2.3 Test Setup

Slabs were tested under the quasi-static punching load applied through a 40 mm diameter cylindrical steel loading rod with hemispherical end. The slabs were clamped on two opposite edges and the load was applied at the centre of slabs. The loaded area was at the centre of rebar mesh (Figure 1) and thus no rebar was in line with the direction of load. It may be noted here that the location of punching load was the one offering least resistance to punching. The load was applied gradually up to the failure of specimens using a hydraulic jack. The loading rate was approximmitly 18 kN per min. The load and displacements were recorded using a data logger. The test setup for the testing of slabs is shown in Figure 4.

## 3 TEST RESULTS AND DISCUSSION

### 3.1 Damage Pattern

The damage on the front face of the slab specimens was almost same for all specimens, as shown in Figure 5(a) for one of the slabs. The damage patterns on the rear face of control, CFRP and TRM strengthened slab specimens are shown in Figures 5(b), 6(a) and 6(b) respectively. The state of damage to concrete in the strengthened slabs was assessed by removing the layers of strengthening material as well as the loose concrete, as shown in Figure 7. The shear cone formation observed in experiments is shown in Figure 8. Examination of concrete shear cone formed in the slabs shows that the shear cone formed in CFRP and TRM strengthened slabs were almost same with the angles $\theta_1$ and $\theta_2$ varying from $60^o$ to $65^o$ and $15^o$ to $20^o$ respectively. Angle $\theta_1$ being close to the value usually adopted by most of the codes, it is taken as $63.4^o$ and the value of angle $\theta_2$ is taken as $20.0^o$ in punching shear calculations presented latter.

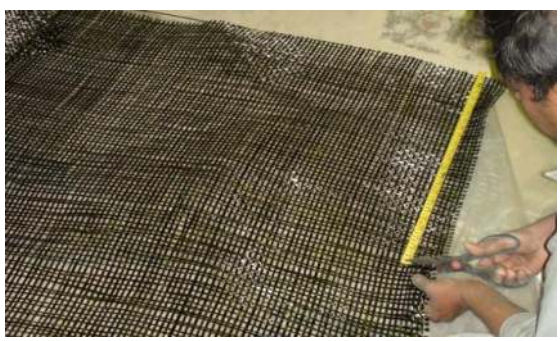

(a) Cutting of TRM fiber



(b) Sika Armatec Epocem application as bonding agent



(c) First layer of Sika Rep mortar application

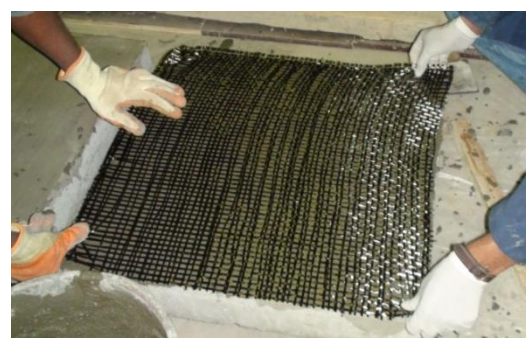

(d) First layer of fabric application



(e) Pressing on fabric for mortar penetration



(f) Saturation of I layer of fabric with mortar

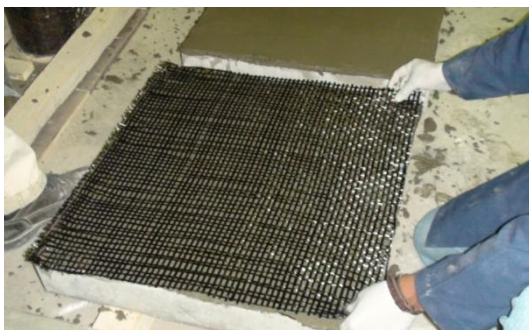

(g) Laying of II layer of fabric



(h) Finished strengthened slab

Figure 3: Step-by-step application of TRM.

### 3.2 Load-Displacement Variation and Energy Absorption

The load-displacement variation for the slabs of two concrete grades A and B is plotted in Figures 9 and 10 respectively. One interesting observation made from these figures is that there are two peak loads for the strengthened slabs. In control slabs, second peak is in the form of a flat or stepped plateau. The second peak load is developed because of the resistance provided by the dowel action of the back face rebars and the strengthening layers.




(a) Full view (b) Close up

Figure 4: Test setup.

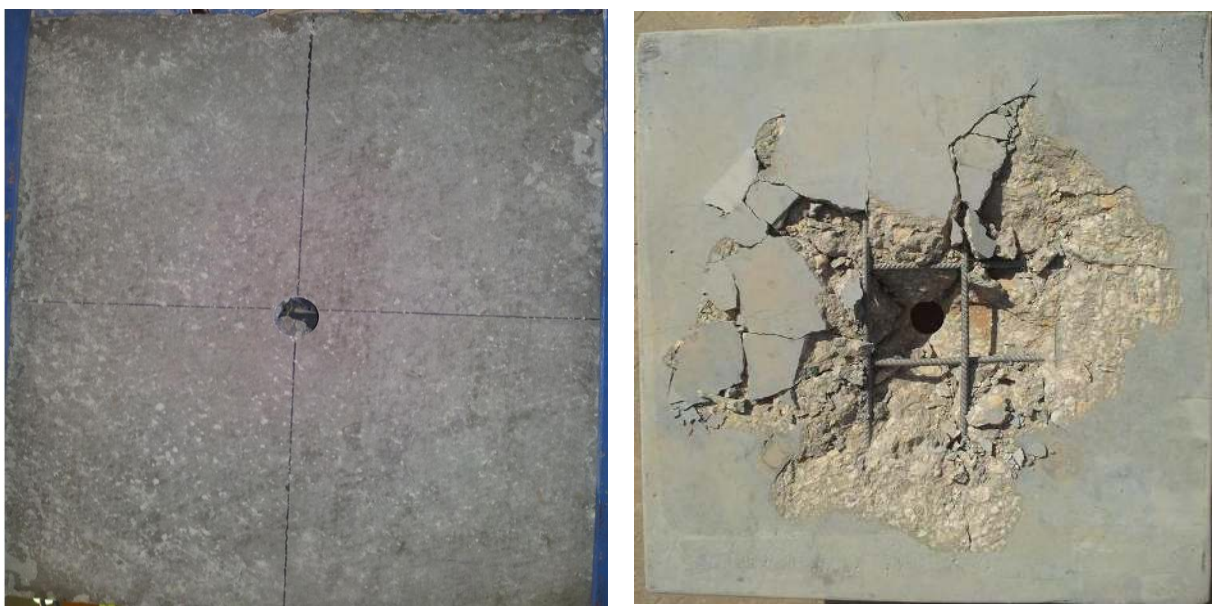

(a) (b)

Figure 5: Punching failure of control slab of concrete grade B: (a) Front face; (b) Back face.




(a) (b)

Figure 6: Punching failure on back face of strengthened slabs of concrete grade B: (a) CFRP strengthened; (b) TRM strengthened.



(a) (b)

Figure 7: Punching failure on back face of strengthened slab of concrete grade B after removing strengthening layer: (a) CFRP strengthened; (b) TRM strengthened.

.

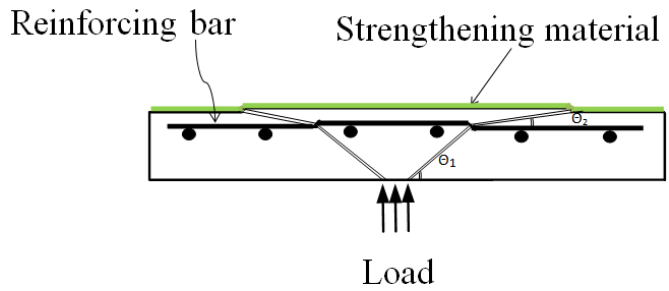


Figure 8: Punching failure model.

Examination of load-displacement curves (Figures 9 and 10) shows that there is a sudden drop in load after reaching its first peak which is due to the start of the formation of shear cone due to which concrete starts losing its punching resistance. It is observed that the peak load is obtained at 4 to 8 mm displacement (after applying zero correction). At the first peak, there were minor cracks most of which were radial on the back face of slab. Though there is sudden drop in load after reaching first peak but the load does not reach the zero level with the same rate of drop. Moreover, there is a significant residual load resistance which remains for considerable displacement and even increases in the strengthened slabs. In control slabs, after post-peak sudden decrease in load, there is a plateau which indicates the resistance provided by the aggregate interlock and the dowel action of rebars in withholding the concrete punch cone. The long plateau in the slab of concrete grade A is due to the brittle failure of concrete whereas for the slab of concrete grade B, it is in steps with short plateaus because of the better bond between concrete and rebars due to the rich concrete grade. In the strengthened slabs, after post-peak drop in load, the load starts rising again due to the resistance provided by the strengthening layers. These observations confirm that the dowel action in the rebars and the strengthening layers start developing after first peak when there has been considerable displacement. This observation is contrary to some of the earlier researches (Reinhartd and Walraven, 1982; Oh and Sim 2004; Rochdi et al., 2006) wherein the dowel action of rebars was added in calculating the punching shear strength (i.e. the first peak load) thereby assuming the development of the dowel action at the peak load. The subsequent punching shear analysis also confirms this observation.

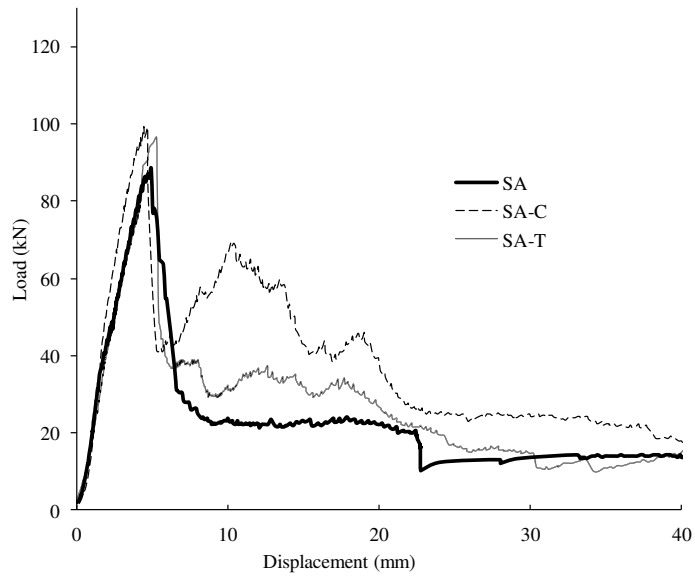


Figure 9: Load-displacement variation for punching of slabs for concrete grade A (SA: control slab; SA-C: CFRP strengthened slab; SA-T: TRM strengthened slab).

The first and second peak loads for different slab types are given in Table 2. The second peak load for the control slabs is taken as the load corresponding to the average plateau height.

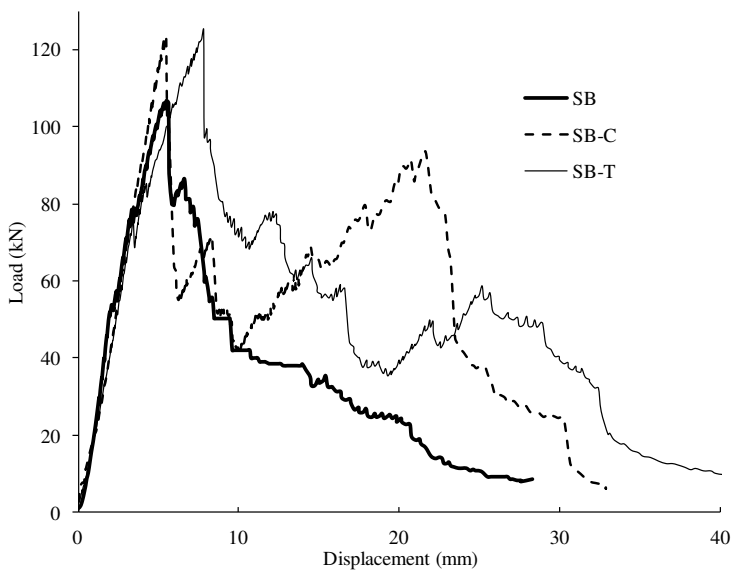


Figure 10: Load-displacement variation for punching of slabs for concrete grade B (SB: control slab; SB-C: CFRP strengthened slab; SB-T: TRM strengthened slab).

| Specimen group ID | Control | | CFRP* | | TRM* | |
|---|---|---|---|---|---|---|
| | I peak | II peak | I peak | II peak | I peak | II peak |
| SA | 88.4 | 24.0 | 99.4 (12.4%) | 69.5 (189.6%) | 96.4 (9.1%) | 37.3 (55.4%) |
| SB | 106.0 | 33.1 | 123.6 (16.6%) | 93.5 (275.5%) | 125.2 (18.1%) | 58.7 (135.7%) |

* Value within brackets is the percentage increase with respect to the control

Table 2: Punching load for different slabs.

It is observed from Figures 9 and 10 that the load-displacement curve for the control and the strengthened slabs is almost same in the beginning but at higher load, the CFRP strengthened slabs show slightly higher stiffness. The effect of strengthening layer is not felt at low magnitude of load whereas at higher magnitude of load, cracks start developing in the control slab and concrete cover starts loosing strength but for the strengthened slabs, besides additional stiffness of strengthening layer, concrete cover also contributes equally especially in CFRP strengthened slabs. It is due to this reason that the CFRP strengthened slabs are stiffer at higher loads close to the first peak. Although the TRM strengthened slabs show almost same stiffness as control due to their low stiffness as compared to CFRP, but the slabs are able to carry more load as compared to the control.

For the CFRP strengthened slabs, although there is a small increase in the first peak load (12.4% for concrete grade A and 16.6% for concrete grade B) but the second peak load is significantly higher (189.6% for concrete grade A and 275.5% for concrete grade B) as compared to the corresponding control slab.

For TRM strengthened slabs, the increase in the first peak load (9.1% for concrete grade A and 18.1% for concrete grade B) is almost same as CFRP strengthened slabs because of the equivalent layers considered for TRM (Al-Salloum et al., 2011). As compared to the control slab, the second peak for concrete grades A and B is 55.4% and 135.7% higher respectively.

The energy absorbed in the quasi-static punching for the two concrete grades A and B is plotted in Figure 11.

The energy absorption is calculated for a displacement up to one-third of the thickness of slab (i.e. 30 mm). This specified value was selected only for comparison because for some slabs load-displacement response could not be recorded beyond this limit. For CFRP strengthened slabs, there is a considerable increase in the energy absorption in the punching of slabs varying from 65.5% to 66.1% for the two concrete grades. For the TRM strengthened slabs, though the first peak load is not affected significantly but the increase in the energy absorption in the punching of slabs varies from 22.0% to 58.7% for the two concrete grades. The significance of the energy absorption in the punching is in giving an idea about the warning available before failure. The enhancement in the energy absorption in the strengthened slabs is mainly due to the formation of the second peak as a

result of the prevention of the movement of punch cone by the strengthening layers. A comparison of the two strengthening schemes in terms of the load-displacement and the energy absorption characteristics shows that the CFRP strengthening is better than TRM strengthening for improving the punching resistance of RC slabs.

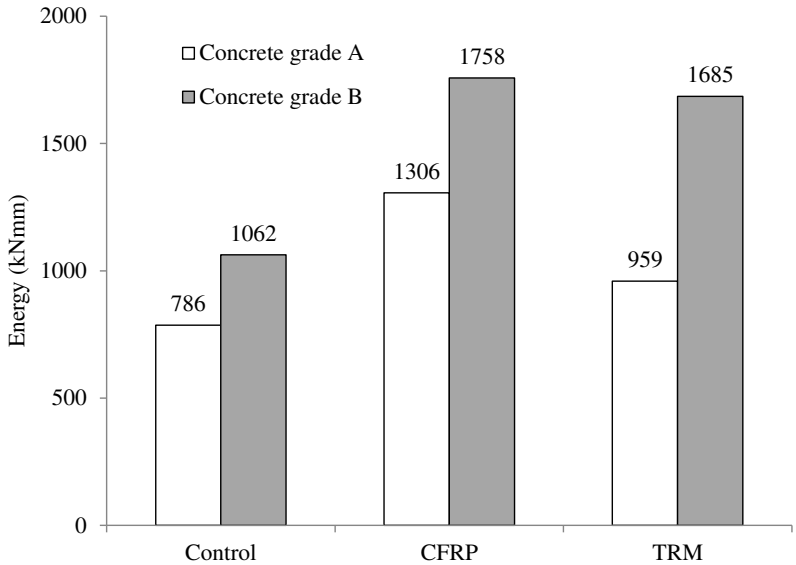


Figure 11: Energy absorption in punching of slabs
(CFRP: CFRP strengthened slab; TRM: TRM strengthened slab).

## 4 PUNCHING SHEAR MODEL

As the steel rod is pushed against the slab, the outer surface of concrete in contact with the rod gets crushed and then the rod penetrates through tunneling which then expands to greater inclination till the level of the rear surface rebars thereby rebars also resist the punching through dowel action. When there is no external strengthening done, the resistance offered by cover concrete is quite less but this gets enhanced considerably in the strengthened slabs. The dowel action provided by the rear surface rebars is dependent on the location and the diameter of the rod.

Besides the resistance offered by concrete, the rear surface rebars offer resistance in the form of dowel action. For the strengthened slabs, the externally bonded CFRP or TRM layers also offer resistance to punching but this comes into action when there has been significant movement of load inside the slab i.e. after crossing the first peak load. When the CFRP or TRM layers start offering resistance, there is again increase in the resistance thus giving rise to the second peak load. The first peak load is estimated from the yield line analysis whereas the second peak load is determined from the residual punching resistance of concrete after the formation of the punch cone and the dowel action provided by the rebars and the strengthening layers.

### 4.1 First Peak Load

The use of externally bonded FRP and TRM layers, employed in this study, results in increasing the flexural capacity of RC slabs which increases the punching capacity as well. The reinforcement and fibers of CFRP and TRM are shown in Figure 1. The moment capacity per unit width of FRP and TRM strengthened slab at an angle $\theta$, $m_\theta$, can be computed using the conventional force and moment equilibrium and strain compatibility across the depth of the slab section as follows:

$$m_\theta = A_s f_y (d - a/2) + A_{fL} \cos^2\theta f_{fL} (D - a/2) + A_{fT} \sin^2\theta f_{fT} (D - a/2) \tag{1}$$

where, $a$ is the depth of stress block given by:

$$a = \frac{A_s f_y + A_{fL} \cos^2\theta f_{fL} + A_{fT} \sin^2\theta f_{fT}}{0.85 f_c^{'} B} \tag{2}$$

in which $A_s$ is the cross-sectional area of the steel rebars used in the slab panel of width $B$; $A_{fL}$ and $A_{fT}$ are the cross-sectional areas of CFRP / TRM strips in the longitudinal and the transverse directions respectively; $D$ is the overall thickness of slab; $d$ is the effective depth of tension steel reinforcement; $f_y$ is the yield stress of reinforcing steel; $f_c^{'}$ is the concrete compressive strength; $f_{fL}$ and $f_{fT}$ are the stresses developed in CFRP / TRM strips at the ultimate strength capacity of the specimens in longitudinal and transverse directions respectively. The stress in the CFRP / TRM strips is the minimum of the stress obtained from the strain compatibility and based on possible delamination failure from the concrete, and is given as:

$$f_f = \min\left(\varepsilon_f E_f, \varepsilon_{fd} E_f, 0.75 f_{fu}\right) \tag{3}$$

where, $\varepsilon_f$ is the strain obtained from strain compatibility ($= \varepsilon_{sy} D/d$); $\varepsilon_{sy}$ is the yield strain of steel; and $\varepsilon_{fd}$ is the CFRP / TRM debonding strain which can be estimated from (Elsanadedy et al. 2014):

$$\varepsilon_{fd} = \left(\frac{\varepsilon_{sy}}{n t_f E_f}\right)^{0.4} \left(6.5 + \frac{n t_f E_f}{135000}\right) \rho_s^{0.05} f_c^{'0.1} \le 0.9 \varepsilon_{fu} \tag{4}$$

where, $\xi_{fu}$ and $f_{fu}$ are the ultimate strain and strength of the CFRP / TRM strips respectively; $t_f$ and $E_f$ represent the CFRP / TRM strip thickness and the modulus of elasticity, respectively; $n$ is the number of layers of CFRP / TRM strips; $\rho_s$ is the reinforcement steel ratio given by:

$$\rho_s = \frac{A_s}{Bd} \tag{5}$$

The average moment capacity per unit width, $m$, of the strengthened slab is calculated as the weighted mean of the slab section along the yield lines:

$$m = \frac{1}{2\pi}\int_{\theta=0}^{2\pi} m_\theta d\theta \tag{6}$$

The variation of $m_\theta$ for the strengthened RC slabs of two concrete grades is shown in Figure 12. The variation of $m_\theta$ is due to the use of single CFRP sheet of unidirectional fibers thus making it orthotropic.

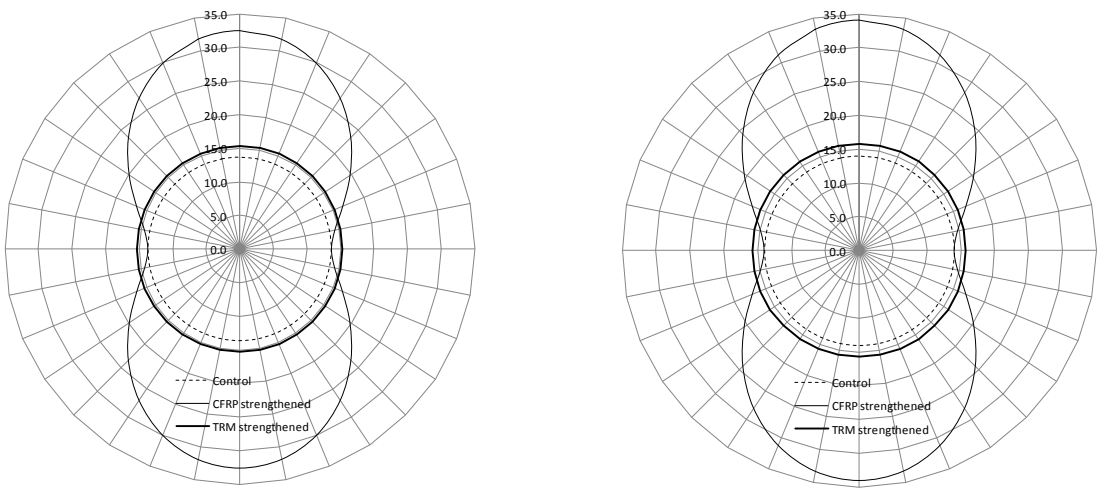


Figure 12: Angular variation of moment capacity of slabs (kNm/m) with CFRP fibers in vertical direction: (a) Concrete grade A; (b) Concrete grade B.

The fibers in the TRM being same in the two orthogonal directions, $m_\theta$ is constant. The flexural capacity of the slab, $P_{flex}$, can be calculated based on the yield line analysis as follows (Elstner and Hognestad, 1956):

$$P_{flex} = 8m\left(\frac{1}{1-c/B} - 3 + 2\sqrt{2}\right) \tag{7}$$

in which $c$ is the side length of equivalent square loaded area.

The punching shear strength, $P_{u1}$, of the strengthened slab is calculated according to the equation proposed by Mowrer and Vanderbilt (1967) as follows:

$$P_{u1} = \frac{0.8(1+d/c)bd\sqrt{f_c^{'}}}{1+0.433bd\sqrt{f_c^{'}}/P_{flex}} \tag{8}$$

where $b$ is the perimeter of the loaded area.

### 4.2 Second Peak Load

The reduction in load after the first peak is due to the start of dislodging of truncated cone thus continuous degradation of shearing resistance offered by concrete which becomes more and more dependent on aggregate interlocking. The movement of cone is then resisted by dowel action provided by steel rebars and CFRP / TRM layers which start building up with increase in the movement of cone thereby leading to the formation of second peak in the strengthened slab. The second peak load is thus the algebraic sum of the resistance offered by concrete after the formation of shear cone through aggregate interlocking and dowel action provided by steel rebars and CFRP /TRM layers:

$$P_{u2} = P_a + P_d \tag{9}$$

where, $P_d$ is the shear resistance provided by dowel action of steel rebars and CFRP / TRM layers; $P_a$ is the shear resistance offered by aggregate interlock in concrete which can be estimated from:

$$P_a = \frac{\alpha}{3}\sqrt{f_c^{'}}b_o D \tag{10}$$

where, $\alpha$ is the shear strength reduction factor due to crack widening/opening at second peak. The value of $\alpha$ is calculated using (Muttoni, 2008).

$$\alpha = \frac{0.75}{1+15\dfrac{\psi d}{d_{g0}+d_g}} \tag{11}$$

where, $d_{g0}$ is 16 mm and $d_g$ is the maximum size of aggregate (= 10 mm in this study); $\psi d$ is the crack width at the second peak. As the second peak occurs when the strengthening material starts offering resistance, its value depends on the strengthening material. The value of $\psi d$ will depend on the stiffness of strengthening material and is expected to be more for TRM as compared to CFRP. For CFRP and TRM strengthened slabs, the value of $\psi d$ is taken as 0.2 and 3.5 mm respectively, whereas its value for control slabs is taken as 9.0 mm. The experimental results of this study support these assumptions.

Hewitt and Batchelor (1975) found the theoretical punching shear strength of RC slabs to be 20% less than the test results which was attributed to the dowel action of the rebars. Regan and Braestrup (1985) stated that the dowel action increased the punching shear strength of RC slab by 34%. In this research, the dowel action hypothesis proposed by Millard and Johnson (1984) and Menerey et al. (1996, 1997) have been modified to include the effect of dowel action provided by CFRP / TRM layers:

$$P_d = P_{ds} + P_{df} = \frac{1}{2}\sum_{i=1}^{n}\phi_i^2\sqrt{f_c^{'}f_y\left\{1-\left(\frac{f_s}{f_y}\right)^2\right\}}\sin\theta_2 + \frac{2A_f}{\pi}\sqrt{f_c^{'}f_{fu}\left\{1-\left(\frac{f_{f1}}{f_{fu}}\right)^2\right\}}\sin\theta_2 \qquad (12)$$

where, $f_s$ is the stress in steel rebars at failure; $\phi_i$ is the diameter of rebars embedded in the punching cone; $n$ is the number of rebars embedded in the punching cone; $f_{f1}$ is the stress in CFRP / TRM at failure; $A_f$ is the cross sectional area of the fibers in CFRP / TRM sheet embedded in the punching cone; $P_{ds}$ is the shear carried by the dowel action of steel rebars; $P_{df}$ is the shear carried by the dowel action of the CFRP/TRM sheets. The above equation shows that a parabolic interaction is assumed between the axial force and the dowel force in the reinforcing bars and fibers of strengthening layers. As the reinforcing bars and fibers of strengthening layers are not at right angle to the punching crack, the dowel contribution is reduced by 50% in the above equation. The stresses in rebars and CFRP /TRM sheet, required in the above equation, can be determined using:

$$f_s = \frac{P_{ds}}{\tan\theta_2\sum_{i=1}^{n}A_{si}} \qquad (13)$$

$$f_{f1} = \frac{P_{df}}{\tan\theta_2 A_f} \qquad (14)$$

where, $A_{si}$ is the area of rebars embedded in the punching cone; $V_{us}$ and $V_{uf}$ are the punching loads shared by steel rebars and CFRP / TRM layers, which have been calculated in proportion to their stiffness, thus giving:

$$P_{df} = \frac{A_f f_{fu} P_d}{\left(A_f f_{fu} + A_s f_y\right)} \qquad (15)$$

$$P_{ds} = P_d - P_{df} \qquad (16)$$

It is seen from the above equations that the stresses $f_s$ and $f_{fl}$ are dependent on the ultimate shear load, which is not known, thus the calculation requires iterations to be carried out for determining the punching load $P_d$.

### 4.3 Comparison of Prediction with Experiments

Based on the above formulation, Tables 3 and 4 present detailed calculations of the first and the second peak loads of the slab specimens tested in the current study. The predicted values of the first peak loads are compared with the experimental values in Table 5, whereas the comparison for second peak is done in Table 4. It can be noted from the tables that the proposed analytical models for the first as well as the second peak loads provide reasonably good predictions for the punching capacity of the tested slabs as the average of the ratio $P_{u\ exp}/P_{u\ \mathrm{model}}$ for the first and the second peaks are 0.90 and 1.02 respectively.

The experimental results of the first peak load or the punching capacity are also compared with ACI 318 (2011) equation for the two-way shear strength:

$$P_u = \frac{1}{6}\left(1+\frac{2}{\beta_c}\right)\sqrt{f_c^{'}}\,b_o d \le \frac{1}{3}\sqrt{f_c^{'}}\,b_o d \tag{17}$$

where $\beta_c$ is the ratio of the long side to the short side of the column, $b_o$ is the perimeter of the critical section for the punching shear taken at a distance of $d/2$ from the periphery of the column.

| Test specimen | Compressive strength of concrete (MPa) | Debonding strain (%) Eq. (4) | Stress in FRP/TRM at failure (MPa) Eq. (3) | Average moment capacity (kNm/m) Eq. (6) | Flextural load, $P_{flex}$ (kN) Eq. (7) | First peak of punching shear load, $P_{u1}$ (kN) Eq. (8) |
|---|---|---|---|---|---|---|
| SA | 39.9 | - | - | 16.2 | 115.6 | 102.5 |
| SA-C | 39.9 | 0.82 | 265 | 26.7 | 192.5 | 109.8 |
| SA-T | 39.9 | 2.20 | 113 | 17.7 | 127.4 | 104.1 |
| SB | 63.2 | - | - | 16.6 | 118.1 | 124.3 |
| SB-C | 63.2 | 0.85 | 265 | 27.6 | 198.7 | 135.1 |
| SB-T | 63.2 | 0.97 | 113 | 31.7 | 228.0 | 137.3 |

Table 3: Punching shear capacity (First peak) prediction using proposed model.

| Test specimen | Crack width at second peak, $\psi d$ (mm) | Shear strength reduction factor, $\alpha$ Eq. (11) | Shear carried by Steel, $P_{ds}$ (kN) Eq. (12, 16) | Shear carried by agg. Interlock, $P_a$ (kN) Eq. (10) | Shear carried by fiber, $P_{df}$ (kN) Eq. (12, 15) | Second peak of punching shear load, $P_{u2}$ (kN) Eq. (9) | Exp/ Predicted |
|---|---|---|---|---|---|---|---|
| SA | 9.0 | 0.12 | 16.3 | 8.0 | 0.0 | 24.2 | 0.99 |
| SA-C | 0.2 | 0.67 | 8.8 | 44.8 | 16.9 | 70.5 | 0.98 |
| SA-T | 3.5 | 0.25 | 13.4 | 16.3 | 4.4 | 34.1 | 1.09 |
| SB | 9.0 | 0.12 | 20.5 | 10.0 | 0.0 | 30.5 | 1.08 |
| SB-C | 0.2 | 0.67 | 11.0 | 21.2 | 21.2 | 89.1 | 1.05 |
| SB-T | 3.5 | 0.25 | 9.3 | 20.5 | 30.7 | 60.5 | 0.97 |
| | | | | | | Average = | 1.02 |

Table 4: Prediction of second peak of punching shear load using proposed model.

| Test Specimen | Punching shear capacity (kN) | | | Comparison with experiments | |
|---|---|---|---|---|---|
| | Experiment | ACI 318 | Proposed model | Exp/ACI | Exp/Model |
| SA | 88.4 | 47.4 | 102.5 | 1.86 | 0.86 |
| SA-C | 99.4 | 47.4 | 109.8 | 2.10 | 0.91 |
| SA-T | 96.4 | 47.4 | 104.1 | 2.03 | 0.93 |
| SB | 106.0 | 59.7 | 124.3 | 1.78 | 0.85 |
| SB-C | 123.6 | 59.7 | 135.1 | 2.07 | 0.92 |
| SB-T | 125.2 | 59.7 | 137.3 | 2.10 | 0.91 |
| Average | | | | 1.99 | 0.90 |

Table 5: Punching shear capacity (First peak) comparison.

| Specimen group ID | Energy absorption* (kN-mm) | | |
|---|---|---|---|
| | Control | CFRP strengthened slabs | TRM strengthened slabs |
| SA | 786 | 1306 (66.1%) | 959 (22.0%) |
| SB | 1062 | 1758 (65.5%) | 1685 (58.7%) |

* Value within brackets is the percentage increase with respect to control.

Table 6: Energy absorption in punching of slabs.

Table 5 shows that ACI equations provide very conservative predictions for the punching shear strength of the tested slabs in comparison to the proposed model. The average ratio $P_{u\ exp}/P_{u\ ACI}$ is 1.99 using the ACI 318 (2011) equation compared to 0.90 for the proposed model as given in Table 5. It should be noted that the code equations do not account for the effect of the strengthening layers and therefore the provisions of the code are not intended for the strengthened slabs. Thus the proposed model may be adopted for the prediction of the punching shear capacity of FRP and TRM strengthened RC slabs.

## 5 CONCLUSIONS

The main findings of the study presented in the paper can be summarized as follows:

i) Experimental load-displacement variations show two peak loads in the strengthened slabs and one peak followed by a plateau in the control slabs. Second peak or the plateau corresponds to the combined action of the aggregate interlock and dowel action of the back face rebars and the strengthening layers. The dowel action of the back face rebars and the strengthening layers had no role in ultimate punching load (i.e. first peak load).
ii) Although the strengthened slabs showed nominal increase in the first peak load (9-18%) but there was significant increase in the second peak load (190-276% for the CFRP strengthened slabs; 55-136% for the TRM strengthened slabs) and energy absorption (˜66% for CFRP strengthened slabs and 22-56% for TRM strengthened slabs).
iii) An analytical model was also developed for predicting the punching shear strength (first and second peaks) of strengthened slabs. The model agrees reasonably well with the experimental results.

### Acknowledgements

The authors gratefully acknowledge the financial grant (No.: ADV 728-02) received from King Abdul-Aziz City for Science and Technology, Saudi Arabia, under National Plan for Science and Technology. Thanks are also extended to the MMB Chair for Research and Studies in Strengthening and Rehabilitation of Structures, at the Department of Civil Engineering, King Saud University for providing technical support.

### References

Abbas, H., Gupta N.K., Alam, M. (2004). Nonlinear response of concrete beams and plates under impact loading. Internatonal ournal of Impact Engineering 30(8-9):1039-1053.

Abdullah, A., Bailey, C.G., Wu, Z.J. (2013). Tests investigating the punching shear of a column-slab connection strengthened with non-prestressed or prestressed FRP plates. Construction and Building Materials 48:1134-1144.

ACI Committee 318 (2011). Building code requirements for reinforced concrete and commentary, ACI 318-11 and 318R-11, Farmington Hills, MI.

Adetifa, B., Polak, M.A. (2005). Retrofit of slab column interior connections using shear bolts. ACI Structural Journal 102(2):268-274.

Alhaddad, M., Siddiqui, N., Abadel, A., Alsayed, S., Al-Salloum, Y. (2012). Numerical investigations on the seismic behavior of FRP and TRM upgraded RC exterior beam-column joints. Journal of Composite for Construction 16(3):308–321.

Al-Rousan, R., Issa, M., Shabila, H. (2012). Performance of reinforced concrete slabs strengthened with different types and configurations of CFRP. Composite Part B: Engineering 43(2):510–521.

Al-Salloum, Y.A., Siddiqui, N.A., Elsanadedy, H.M., Abadel, A.A., Aqel, M.A. (2011). Textile-reinforced mortar (TRM) versus FRP as strengthening material of seismically deficient RC beam-column-joints. Journal of Composite for Construction 15(6):920–933.

ASTM. (1985). Method for tensile strength of hydraulic cement mortars. C190-85, West Conshohocken, PA.

ASTM. (2002). Standard test method for compressive strength of hydraulic cement mortars (Using 2-in. or [50-mm] Cube Specimens). C109/C109M-02, Annual book of ASTM standards, Vol. 4.01, West Conshohocken, PA.

ASTM. (2012). Standard test method for compressive strength of cylindrical concrete specimens. C39/C39M.,Annual Book of ASTM Standards, 04.02, West Conshohocken, PA

ASTM. (2012). Standard test methods and definitions for mechanical testing of steel products. A370-12, West Conshohocken, PA.

Binici, B., Bayrak, O. (2003). Punching shear strengthening of reinforced concrete flat plates using carbon fiber reinforced polymers. Journal of Strucural Engineering 129(9):1173–1182.

Cantwell, W.J., Smith, K., (1999). The static and dynamic response of CFRP-strengthened concrete structures. Journal of Material Scince Letters 18:309-310.

Chen, C.C., Li, C.Y. (2000). Experimental study on the punching shear behaviour of RC slabs. Proc., International Workshop on Punching Shear Capacity on RC Slabs, Royal Institute of Technology, Stockholm, Sweden 415-422.

Chen, C.C., Li, C.Y. (2005). Punching shear strength of reinforced concrete slabs strengthened with glass fiber-reinforced polymer laminates. ACI Structural Journal 102(4):535-542.

Cheng, C., Chung, L. (2005). Punching shear strength of reinforced concrete slabs strengthened with glass fiber-reinforced polymerlaminates. ACI Structural Journal 102(4):535-542.

Ebead, U., Marzouk, H. (2002). Strengthening of two-way slabs using steel plates. ACI Structural Journal 99(1):23–30.

Ebead, U., Marzouk, H. (2004). Fiber-reinforced polymer strengthening of two-way slabs. ACI Structural Journal 101(5), 650–659.

El-Salakawy, E., Soudki, K.A., Polak, M.A. (2004). Punching shear behavior of flat slabs strengthened with fiber reinforced polymer laminates. Journal of Composite for Construction 8(5):384–92.

Elsanadedy, H.M., Abbas, H., Al-Salloum, Y.A., Almusallam, T.H. (2014). Prediction of intermediate crack debonding strain of externally bonded FRP laminates in RC beams and one-way slabs. Journal of Composite for Construction. DOI: 10.1061/(ASCE)CC.1943-5614.0000462. 18(5):04014008.

Elsanadedy, H.M., Almusallam, T.H., Abbas, H., Al-Salloum Y.A., Alsayed, S.H. (2011). Effect of blast loading on CFRP-retrofitted RC columns – A Numerical Study. Latin American Journal of Solids and Structures 8(1):55-81.

El-Sayed, A.K. (2014). Strengthening of structurally damaged wide shallow RC beams using externally bonded CFRP plates. Latin American Journal of Solids and Structures 11(6):946-965.

Elstner, R.C., Hognestad, E. (1956). Shearing strength of reinforced concrete slabs. ACI Journal Proceeding 53(2):29-58.

Erki, M.A., Heffernan, P.J. (1995). Reinforced concrete slabs externally strengthened with fibre reinforced plastics materials. Proceeding of 2nd International Symposium on Non-Metalic FRP Reinforcement for Concrete Structures (FRPRCS-2), L. Taerwe, ed., E & FN Spon, London, 509–516.

Esfahani, M., Kianoush, M., Moradi, A. (2009). Punching shear strength of interior slab–column connections strengthened with carbon fiber reinforced polymer sheets. Engineering Structure 31(7):1535-1542.

Farghaly, A.S., Ueda, T. (2011). Prediction of punching shear strength of two way slabs strengthened externally with FRP sheets. Journal of Composite for Construction 15(2):181–193.

Gardner, N.J., Huh, J., Chung, L. (2002). Lessons from the sampoong department store collapse. Cement and Concrete Composite 24(6):523-529.

Ghali, A., Sargious, M.A., Huizer, A. (1974). Vertical prestressing of flat plates around columns. Shear in reinforced concrete, ACI SP, SP-42, 2: 905–920.

Harajli, M.H., Soudki, K.A. (2003). Shear strengthening of interior slab-column connections using carbon fiber-reinforced polymer sheets. Journal of Composite for Construction 7(2):145–153.

Hassanzadeh, G., Sundqvist, H. (1998). Strengthening of bridge slabs on columns. Nordic Concrete Research: The Nordic Concrete Federation, publication no. 21; 1998. Paper no. 2.

Hewitt, B.E., Batchelor, BdeV. (1975). Punching shear strength of restrained slabs. Journal of Structural Division 101(9):1837–53.

Kim, D., Sebastian, W.M. (2002). Parametric study of bond failure in concrete beams externally strengthened with fiber reinforced polymer plates. Magazine of Concrete Research 54 (1):47-59.

Koppitz, R., Kenel, A., Keller, T. (2013). Punching shear of RC flat slabs – Review of analytical models for new and strengthening of existing slabs. Engineering Structural 52:123-130.

Limam O., Nguyen, V.T., Foret G. (2005). Numerical and experimental analysis of two-way slabs strengthened with CFRP strips. Engineering Structure 27(6): 841-845

Malvar, L.J., Warren, G.E., Inaba, C.M. (2000). Large scale tests on Navy reinforced concrete pier decks strengthened with CFRP sheets. Proceeding of 3rd International Conference on Advanced Composite Materials in Bridges and Structures, ACMBS-III, Canadian Society for Civil Eng., Montreal, Quebec, 497-504.

Meier, U. (1992). Carbon fibre-reinforced polymers, Modern materials in bridge engineering. Structural Engineering International 2(1):7-12.

Menerey, Ph., (1996). Analytical computation of the punching strength of reinforced concrete. ACI Structural Journal 93(5):503–11.

Menerey, Ph., Walther, R., Zimmermann, Th. (1997). Simulation of punching failure in reinforced-concrete structures. Journal of Structural Engineering 123(5):652–9.

Millard S.G., Johnson, R.P. (1984). Shear transfer across cracks in reinforced concrete due to aggregate interlock and dowel action. Magazine of Concrete Research 36(126):9–21.

Mowrer, R.D., Vanderbilt, M.D. (1967). Shear strength of light-weight aggregate reinforced concrete flat plates. ACI Journal Proceeding 64(11):722-729.

Muttoni, A. (2008). Punching strength of reinforced concrete slabs without transverse reinforcement. ACI structural Journal 105(4):440-450.

Oh, H., Sim, J. (2004). Punching shear strength of strengthened deck panels with externally bonded plates. Composite Part B 35(4):313–321.

Papanicolaou, C., Triantafillou, T., Papantoniou, I., Balioukos, C. (2009). Strengthening of two-way reinforced concrete slabs with textile reinforced mortars (TRM). Proceeding of 4th colloquium on textile reinforced structures (CTRS4), Dresden. Technische Universität Dresde.

Peled, A., Mobasher, B. (2007). Tensile Behavior of Fabric Cement-Based Composites: Pultruded and Cast, ASCE Journal of Materials in Civil Engineering 19(4):340-348.

Arboleda, D., Loreto, G., De Luca, A., Nanni, A. (2012). Material characterization of fiber reinforced cementitious matrix (FRCM) composite laminates. Proceedings of 10th International Symposium on Ferrocement and Thin Reinforced Cement Composite, Havana, Cuba, October 12-17.

RILEM TC 201TRC (2006). Textile Reinforced Concrete State of the art Report of RILEM TC.

Regan, P.E., Braestrup, M.W. (1985). Punching shear in reinforced concrete. Bulletin d'Information 168, Comitte Euro-International du Beton.

Reinhartd, H.W., Walraven, J.C. (1982). Crack in concrete subject to shear. Journal of Structural Divison 108(ST1):207–224.

Rochdi, E.H., Bigaud, D., Ferrier, E., Hamelin, P. (2006). Ultimate behavior of CFRP strengthened RC flat slabs under a centrally applied load. Composite Structures 72(1):69–78.

Sharaf, M., Soudki, K., Van Dusen, M. (2006). CFRP strengthening for punching shear of interior slab–column connections. Journal of Composite for Constuction 10(5):410–418.

Siddiqui, N.A. (2011). Experimental investigation of RC beams strengthened with externally bonded FRP composites. Latin American Journal of Solids and Structures 6(4):343-362.

Soudki K., El-Sayed A.K., Tim Vanzwol, T. (2012). Strengthening of concrete slab-column connections using CFRP strips. Journal of King Saud University- Engineering Science 24:25–33.

Triantafillou, T.C., Papanicolaou, C.G. (2006). Shear strengthening of reinforced concrete members with textile reinforced mortar (TRM) jackets. Material and Structure 39(1):93–103.

Triantafillou, T.C., Papanicolaou, C.G., Zissimopoulos, P., Laourdekis, T. (2006). Concrete confinement with textile-reinforced mortar jackets. ACI Structural Journal 103(1):28–37.

Van Zowl, T., Soudki, K. (2003). Strengthening of concrete slabcolumn connections for punching shear. Technical Report, University of Waterloo, Waterloo, Canada.

Wang, J.W., Tan, K.I. (2001). Punching shear behaviour of RC flat slabs externally strengthened with CFRP system. Proc., 5th Int. Conf. on Fibre-Reinforced Plastic for Reinforced Concrete Structures (FRPRCS-5), Vol. 2, Thomas Telford, London, 997–1005.